Journal of Engineering and Sustainable Development
Vol. 29, No. 05, *August* 2025
https://jeasd.uomustansiriyah.edu.iq/index.php/jeasd
ISSN 2520-0917
Research Article
https://doi.org/10.31272/jeasd.2864

Time series analysis of vegetation index and land degradation assessment in Dhi Qar governorate (Iraq)

Mohammed H. Azeez[1,2*], Hisham M. Jawad Al Sharaa[2], Abdul Razzak T. Ziboon[3]

[1]Department of Surveying, Shatrah Technical Institute (STI), Southern Technical University (STU), Shatrah, Iraq
[2]Department of Civil Engineering, College of Engineering, University of Technology, Baghdad, Iraq
[3]Department of Building and Construction Technology, College of Engineering, Al-Esraa University, Baghdad, Iraq

[*]Email: mohammed.aziz@stu.edu.iq

Article Info

Received 20/07/2024
Revised 11/05/2025
Accepted 01/06/2025

Abstract

Land degradation is a complex problem involving many factors, and it is a change in the land over time. The loss of vegetation cover or a decrease in productivity is one of the indicators of land degradation. This research analyzes vegetation health and density measures using time series analysis of the Normalized Difference Vegetation Index (NDVI) extracted from Landsat 8 satellite data. The study employs the Mann-Kendall (MK) test and Simple Linear Regression (SLR) to identify trends. Additionally, the Bayesian Estimator of Abrupt Change, Seasonality, and Trend model (BEAST) was used for its advantages in trend analysis and change point detection in the study area of Dhi Qar, Iraq. The analysis indicates a decline in the NDVI trend. However, the BEAST method showed its distinction in revealing the details of the trend analysis and change points. In 2022, NDVI declined sharply, with vegetation cover loss estimated at 47% compared to 2014. Maps showing spatial distribution between 2014 and 2023 highlighted this change, which was linked to alterations in rainfall patterns. Therefore, we conclude that meteorological drought strongly affects the vegetation cover in the study area, and repeated drought leads to the loss of vegetation cover and, consequently, to land degradation.

Keywords: Iraq-Dhi Qar, Land degradation, Spatiotemporal analysis, Time series.

1. Introduction

Land degradation is the decline in land productivity over time, posing a significant obstacle to sustainable development. It is a complex issue with numerous contributing factors and no single standard for its detection [1]. The complexity of land degradation lies in the fact that it has multiple sources or factors. The complexities of land degradation are due to various sources, classified into five components: Soil Degradation, Vegetation Degradation, Water Degradation, Climate Degradation, and Losses to Urban/Industrial Development. Moreover, the complexity of the problem of land degradation is that it occurs over time and space slowly and constantly. Although the problem of land degradation is complex, the change in vegetation cover is evidence of it, and remote sensing techniques (RE) can be used to provide a vegetation coverage index [2],[3].

The RE is a powerful technique for detecting and monitoring vegetation changes [4],[5], as time series analysis has been used in many studies in different environments [6]-[8]. RE techniques allow researchers to study phenomena that change over time and space (e.g., land degradation) [9]. Therefore, many studies applied time series analysis of the Normalized Difference Vegetation Index (NDVI). Some of these studies relied on NDVI to detect changes over time in vegetation density, in addition to climate data [10]. At the same time, other studies relied on NDVI only [11]. Ziboon et al. [9] used RE techniques and geographic information systems (GIS) to research degradation in the Mesopotamian region. They used NDVI as an indicator to identify changes in vegetation cover in the area. Rasheed [12]also employed RE techniques and GIS to detect the impact of climate change on desertification and the formation of dunes east of the Tigris River in Salah Al-Din Governorate. Attafi et al [10] compared NDVI and Standardized Precipitation Index (SPI)to assess drought and detect drought in a study area in Basra, where drought is considered one of the causes of degradation. These previous studies used RE techniques and GIS to detect vegetation cover changes in specific areas of Iraq, and some studies provided a comprehensive analysis of vegetation cover using the same RE techniques as Abbas et al. [13] analyzed time series of vegetation cover for all of Iraq. The method or technique used

was unclear, but it indicated a decline in the trend of vegetation cover. Hatem et al. [11] also used NDVI as a drought indicator for Iraq and analyzed the NDVI time series from 2000 to 2022. The basis of their analysis was a visual analysis of the graphs they produced. In addition to the studies that have focused on analyzing the change in the vegetation cover in Iraq overall, we have found only a small number of studies specific to the Dhi Qar region, to the best of our knowledge. Hassan and Dakheel [14] chose specific years to assess the vegetation cover. Concurrently, Hashoush [15] conducted a change detection analysis of the vegetation cover in Dhi Qar Governorate for 2013 and 2022.

The researchers found severe vegetation degradation throughout Iraq, particularly in the Dhi Qar study area. In previous studies, more precise methods have been needed to represent trends in both temporal and spatial dimensions. Our research seeks to address this gap by conducting a time series analysis in the Thi Qar study area. This analysis has been the first of its kind. It involves the application of three different methods: simple linear regression (SLR), the Mann-Kendall (MK) test for non-parametric data, and the Bayesian Estimator of Abrupt Change, Seasonality, and Trend (BEAST). Additionally, we have created maps depicting changes in vegetation cover over time and space. These methods have been instrumental in demonstrating land degradation in Thi Qar.

2. Materials and Methods

2.1. Study area

The focus of this study is Dhi Qar governorate, which extends from Wasit governorate in the north to Basra governorate in the south and from Maysan governorate in the east to Al-Muthanna governorate in the west of Iraq. The study area is located between latitudes 30° and 32° North and longitudes 45° and 47° East. The governorate is approximately 161.5 km long and has a width ranging from 55 km to 142 km. The study area of Dhi Qar is a diverse area that includes marshes, wetlands, agricultural areas, and grazing areas. It is valuable due to its archaeological and tourist sites. See Fig.1.

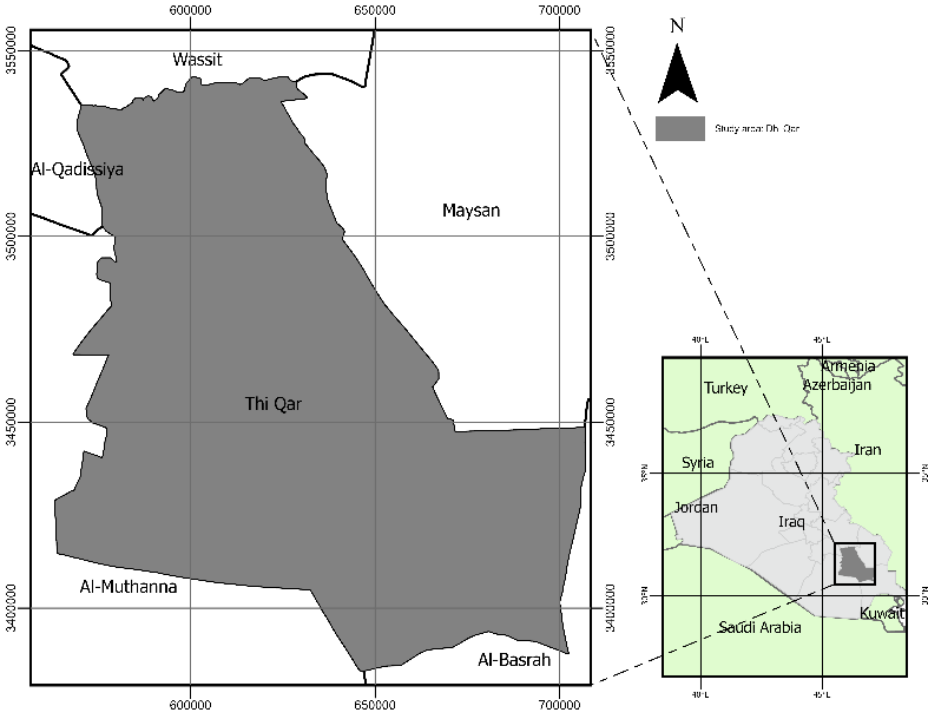

Figure 1. Shows the study area (not to scale).

2.2. The Data and Pre-processing.

The NDVI data were obtained for the time series from 2014 to 2023. It was extracted from Landsat 8 satellite images. Top-of-atmosphere reflectance (TOA) images had 0% cloud cover. The data was accessed using the Google Earth Engine platform (GEE: http://Earthengine.google.com), which is considered the best and fastest platform for analysing spatial data and satellite data [16].

Rainfall data was obtained from four Ground Weather Stations(GWS's) located throughout the study area. These data were recorded between 2014 and 2022 (see Fig. 2 and Fig. 3). Notably, the website of the Iraqi Ministry of Agriculture (http://www.agromet.gov.iq/) provides access to daily climate data.

Rainfall data from GWS still represent a single point and not a surface (raster data), so they must be interpolated using one of the interpolation techniques, such as Kriging and Inverse Distance Weighting (IDW). Kergen is a stochastic method and does not require prior knowledge about the phenomenon to be represented as a surface. In return, it requires more parameters, unlike IDW. IDW is a simple deterministic method that requires prior knowledge about the phenomenon to be represented as a surface[17]-[18]. Since we have previous knowledge about the location of GWSs and the distance between the stations that

control the formation of the surface, IDW was the best for a surface that represents rainfall from GWS's data.

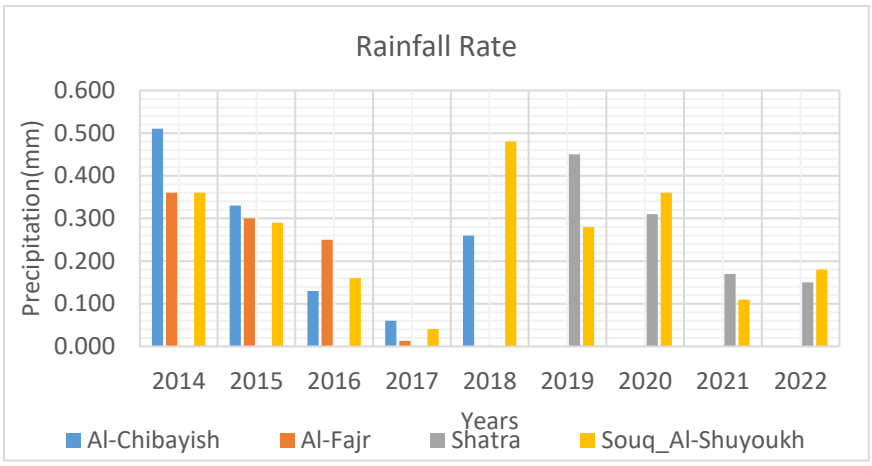

Figure 2. Showing the rate of rainfall in Dhi Qar Governorate. Data were collected from four geoclimatic monitoring stations.

A raster was created using IDW techniques from data collected at the four WGSs ("Shatra," "Al-Fajr," "Souq_Al-Shuyoukh," and "Al-Chibayish"). The raster has a cell size of 300 x 300 m (refer to Fig.3). This process was carried out using the ArcGIS software package.

2.3. Time series datasets

The NDVI time series was decomposed using the BEAST model. This decomposition aims to determine the year in which a change in vegetation cover occurred in the Dhi Qar Governorate and then choose that year as the reference for creating spatial maps.

BEAST decomposes the time series into its trend, seasonal, and remainder components. However, the model structure, or the number and timing of breakpoints, is estimated through Bayesian modeling to reduce uncertainty, overfitting, and model misspecification. This model was formulated by Zhao et al [19]. The BEAST model was used with remote sensing data for time series analysis [20]-[22].Many other studies in various fields, for example, in ecology [23], in environmental engineering [24], in biomedical engineering [25], in geography [26], and in watershed hydrology [27]. The power of the BEAST model is in revealing the local trend between periods, providing a reasonable interpretation of vegetation change in the study area. BEAST formulated are:

$$Y_t = T(t_i; \Theta_T) + S(t_i; \Theta_s) + \varepsilon_i \quad (1)$$

Where Y is the observed data at time t (t = 1, …n), i is the index of the time dimension, T is the trend component, and it is a piecewise linear model with m breakpoints and m + 1 linear models, where abrupt changes are found at the breakpoints τi (i = 1, …m) and gradual changes are given by the:

$$T = \alpha, + \beta_i t \quad (2)$$

S is the seasonal component, fit with a harmonic model with ρ breakpoints and ρ + 1 harmonic models, where seasonal changes are found at the breakpoints ξj (j = 1, … ρ). Harmonic models account for periodicity using K harmonic terms (sinusoids with different characteristics):

$$S_i = \sum_{k=1}^{k} \varphi_{j.k} \sin\left(\frac{2\pi kt}{f} + \delta_{j,k}\right) \quad (3)$$

For $\xi j - 1 \leq t < \xi j$, where φ is the amplitude, f is the frequency, and δ is the phase of the sine wave. (3) has been modified to be compatible with BEAST for handling nonlinear time series such as the NDVI time series:

$$S_i = \sum_{k=1}^{k} \left[\gamma_{j.k} \sin\left(\frac{2\pi kt}{f}\right) + \theta_{j.k} \cos\left(\frac{2\pi kt}{f}\right)\right] \quad (3b)$$

Where the linear coefficients of the regression model are $\gamma j,k = \varphi j,k cos\delta j,k$ and $\theta j,k = \varphi j,k sin\delta j,k$, note that K is a user-defined constant (it does not vary across j segments). ε_i is the remainder component. The trend component linear model: Θ_T represents the parameters related to the trend, and Θ_S represents the parameters related to seasonality. It is expressed in the following:

$$\Theta_T = \{m\} \cup \{\tau_I\}_{i=1,\ldots.m} \cup \{\alpha, \beta_i\}_{i=0,\ldots.m} \quad (4)$$

$$\Theta_s = \{p\} \cup \{\xi\}_{j=1,.p} \cup \{k\}_{j=0,..p} \cup \{\gamma_{j,k}, \theta_{j,k}\}_{j=0,.p;k=1.,k_j} \quad (5)$$

Reformulating (1) as a simple linear regression:

$$Y_t = X_M(t_i)\beta_m + \varepsilon_i \quad (6)$$

Where X_M is the design matrix with the form dependent on M, and M is the model structure from (4) and (5):

$$M = \{m\} \cup \{\tau_I\}_{i=1,\ldots.m} \cup \{p\} \cup \{\xi\}_{j=1,\ldots.p} \cup \{k\}_{j=0,\ldots.p} \quad (7)$$

And β_m are the corresponding coefficients from (4) and (5):

$$\beta_M = \{\alpha, \beta_i\}_{i=0,\ldots.m} \cup \{\gamma_{j,k}, \theta_{j,k}\}_{j=0,\ldots.p;k=1.,\ldots.k_j} \quad (8)$$

The Google Colab platform was used to implement this model after preparing the necessary data and libraries. The library that contains the code for this model is Rbeast [28]. The full description of the BEAST model can be found at [19].

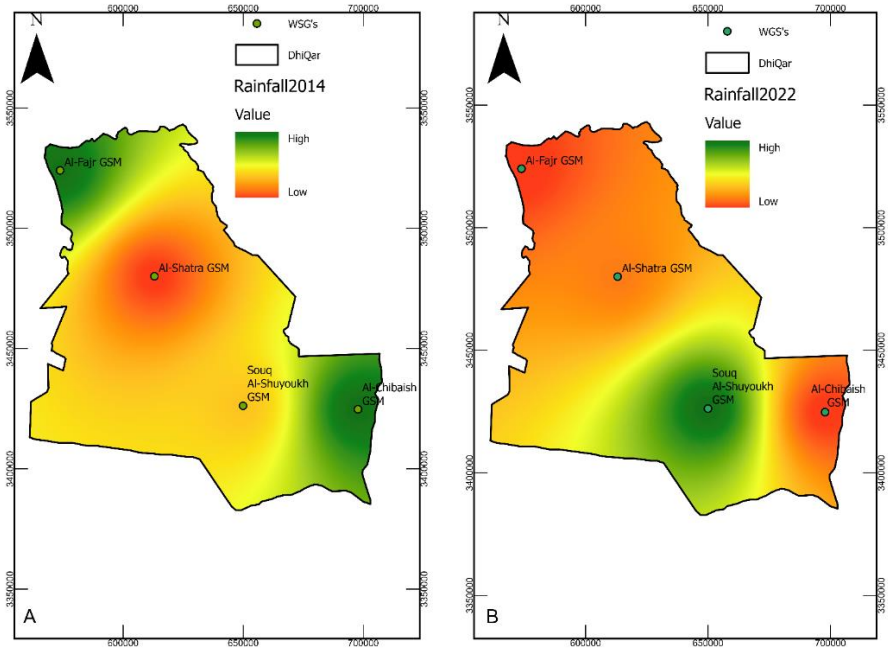

Figure 3. The spatial distribution of rainfall amounts in the study area and the locations of GWSs using the IDW method. (A) 2014 February. (B) 2022, February. (All figures are not to scale.)

2.4. The Mann-Kendall (MK) test

The MK test is widely used to measure a trend in time series extracted from remote sensing techniques [29]-[31]. The NDVI time series often violates parametric assumptions, such as normality and homoscedasticity [32]-[34]. Since they are considered non-parametric values, choose an appropriate MK test for this task [31], [34]. We used the MK test to answer the following question (Is there a trend in vegetation cover change in the study area? Is it a negative or positive trend?). According to the following equations that explain this test [29], [32]:

$$s = \sum_{k=1}^{n-1} \sum_{k+1}^{n} sgn(x_j + x_k) \quad (9)$$

Where

$$sgn(x_j + x_k) = \begin{cases} -1\,, x_j + x_k < 0 \\ 0\,, x_j + x_k = 0 \\ 1\,, \; x_j + x_k > 0 \end{cases} \quad (10)$$

The symbol S indicates the MK test, while Xj and Xk are the sequential values; n is the length of the data series. The variance of S and the standardized Z test statistic are given by the following:

$$\mathrm{Var(s)} = \frac{\mathrm{n(n-1)(2n+5)} - \sum_{\mathrm{p=1}}^{\mathrm{g}} \mathrm{t_p(t_p-1)(2t_p+5)}}{18} \quad (11)$$

$$\mathrm{Z} = \begin{cases} \frac{\mathrm{s-1}}{\sqrt{\mathrm{Var(s)}}}, & \mathrm{s} > 0 \\ 0, & \mathrm{s} = 0 \\ \frac{\mathrm{S+1}}{\sqrt{\mathrm{Var(s)}}}, & \mathrm{s} < 0 \end{cases} \quad (12)$$

Where n is the number of data points, g is the number of tied groups, and Z statistic fits the standard normal distribution. A positive value of Z means there is a change with an upward trend, while a negative value means there is a decreasing or declining trend [35].

The trend of the time series of NDVI was tested using the MK test. This test gives us a general idea of the trend of vegetation change in the study area. This test is suitable for non-parametric data obtained from remote sensing [36]-[40]. However, SLR was applied to test the slope during the period of the study. The Python programming language was used on the Google Colab platform to conduct the MK, and the non-parametric MK family package [41] was used.

3. Results and Discussion

3.1. Check the Change Points in the NDVI time series

The BEAST model was tuned to achieve the best performance for detecting Changepoints in the NDVI time series from 2014 to 2023. The NDVI time series shows seasonal patterns, and the Single-Value Decomposition (SVD) method was selected to identify these seasons. The SVD-based basis functions are more economical than the harmonic sine/cosine bases in capturing seasonal variations, making it more likely to detect subtle changes. The results of the BEAST model showed that the 8 Changepoints with the highest probability of Changepoint (PCP) were in the years 2014 and 2022, with PCPs of 0.99 and 0.98, respectively (See Table 1). Based on the BEAST model's results, slices were taken from the NDVI time series (see Fig. 4 and Fig.5). These slices have been used to produce spatial distribution maps of the NDVI. Since 2022 is the year in which the most change and decline in trend occurred in the value of NDVI, it was considered a year compared to the beginning of the time series in 2014 and the end of the time series in 2023. These NDVI distribution maps were produced from Landsat 8 satellite data.

3.2. The trend of vegetation change

The MK test showed a definite decline in NDVI from 2014 to 2023. The decline index was (-3.19*10^-5) at the confidence level of 95, and the P-value was (5.875*10^-5). Likewise, SLR

shows the same results. See Table 2 and Fig. 6. Using SLR, the time series analysis of NDVI showed a decrease of (-3.3*10^-5), identical to the MK test. The rate of change per pixel was -0.0018. The prediction accuracy was with a mean absolute presetting error (MAPE) of 20%. Also, the mean absolute deviation (MAD) and the mean squared error (MAE) were 0.0335 and 0.0026, respectively.

Table 1. The probability of a Changepoint (PCP)occurring and the probability of a Changepoint (PCPT)occurring in the trend.

Time	PCP	Time	PCPT
2022	0.99175	2019	0.97842
2014	0.98621	2023	0.94538
2015	0.97029	2021	0.81025
2019	0.85863	2015	0.69346
2017	0.75854	2016	0.58946
2023	0.54263	2023	0.45810
2018	0.41708	2017	0.38263
2020	0.07796	2020	0.32396

In addition to trend analysis using MK and SLR, the BEAST model can analyze trends between two time periods and detect change points in the time series. The BEAST results showed eight trend change points, with the highest PCPT occurring in 2019 at 0.97. There was an increase in the trend component (TC) and probabilities of the slope (PS) in 2019. However, by the end of 2020, a sharp decline in TC and PS was observed. This decline is expected to continue until the beginning of 2023. Table 1 and Fig. 5. In 2023, PC and PT were 0.945, with a slight increase in TC and PS. Along the NDVI time series, there is a fluctuation in the TC and PS since 2014, but 2022 is the lowest value of the TC and PS. This gives another reason for choosing the year 2022 as a reference year.

3.3. Areas of vegetation cover for reference years and forward and backward years

The area covered by vegetation was 174079 hectares in 2014. This area decreased by 47% to reach 62722 hectares in 2022 (See Fig.7). A decrease in rainfall accompanied this decrease in vegetation cover, as the amount of rainfall in 2022 did not exceed 15 mm in the entire study area (note Fig. 2 and 4A).

As illustrated in Fig. 3, the spatial distribution of rainfall was uneven, which significantly influenced vegetation cover. Unfortunately, ground-based meteorological stations did not provide rainfall data for the year 2023. However, there was a notable 28% increase in vegetation cover compared to 2022, with the total area reaching 112,418 hectares, as shown in Fig. 7. It is important to note that this increase in vegetation cover between 2022 and 2023 does not necessarily indicate that the land has been fully restored to its original health; this issue will be addressed in the subsequent paragraph.

The study area experienced a significant increase in vegetation cover in 2014, which extended across most of the region. However, by 2022, the vegetation cover had decreased slightly towards the centre of the area. This is because the centre of the region is primarily used for agriculture and relies on irrigation from rivers. See Fig. 8 (A, B, and C). Comparing the years 2023 and 2014, the vegetation cover mostly declined in the east and west of the study area. These lands, due to the wave of rainfall shortage, did not regain vegetation cover in 2023. See Fig. 8 (D).

Table 2. Mann Kendall Test

Determinants	value
Trend	decreasing
h	True
p	5.8757969456424e-05
z	-4.017744044969664
Tau	-0.10831280951245995
s	-20450.0
var_s	25904762.6666666
slope	-3.1963470319634e-05
intercept	0.17781278538812786

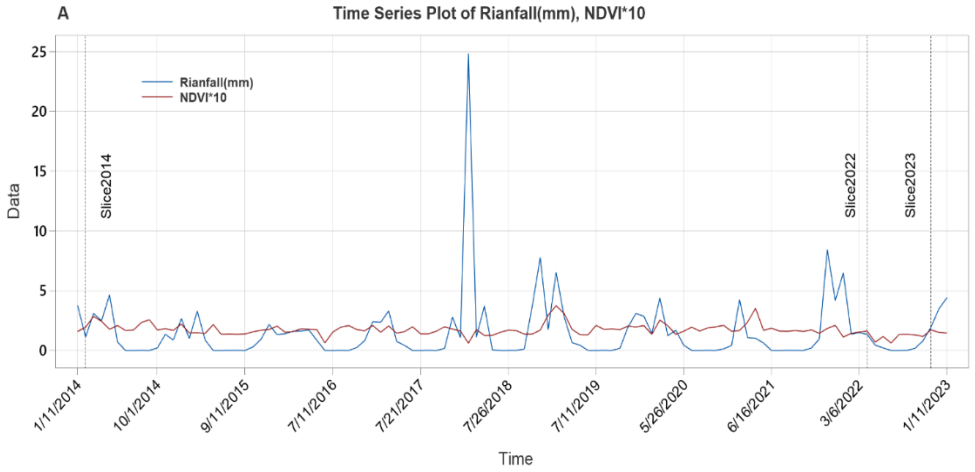

Figure 4. The smoothing of time series and removing noise for the NDVI using the Moving Average method. (A) And a time series of rainfall amounts. Slices of the NDVI time series were also enlarged. (B) Slice 2014, (C) Slice 2022, and (D) Slice 2023. Based on these slides, maps of the spatial distribution of vegetation cover will be produced.

3.4. Discussion

The vegetation cover in Dhi Qar Governorate fluctuated over ten years, as NDVI fluctuated, accompanied by rainfall fluctuations in the study area. This rainfall and NDVI fluctuation is almost consistent, indicating a relationship between rainfall and vegetation cover (see Figs. 2 and 4A). Since meteorological drought is a lack of rainfall, it can be expressed that the vegetation cover in the Dhi Qar Governorate is affected by meteorological drought. This hypothesis is confirmed by [11], [42], [43]. They confirmed the occurrence

of meteorological drought in the years 2015, 2017, and 2022, which is consistent with the results we obtained from the BEAST model. The BEAST model confirmed that the years of the change points in the NDVI time series were 2015, 2017, and 2022 (see Fig. 5 and Table 1).

The NDVI values declined after 2019, with the most significant drop in 2022. Also, the lowest recorded rainfall value in 2022 was in the study area, indicating the presence of severe meteorological drought. The spatial distribution map of NDVI in 2022 showed scattered vegetation cover in the middle of the study area, which is considered an agricultural area (see Fig. 8D). The temporal distribution of NDVI also confirms this matter. The highest NDVI value recorded was 0.20 in March 2022, indicating weak or scattered vegetation cover (refer to Fig. 3C). Trend analysis using MK and SLR gave a negative slope for the NDVI time series. In addition, the TC and PC analysis in the BEAST model provided more accurate details about the trend (see Figs . 5 and 6). The evidence indicates a decrease in the value of NDVI, which suggests the likelihood of land degradation. Shnichal et al. [44]confirmed this by identifying a reduction in vegetation cover in the Dhi Qar study area since 2010.

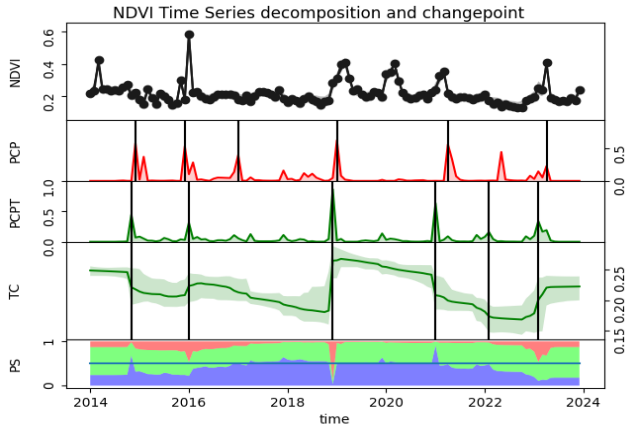

Figure 5. NDVI Time Series decomposition and changepoint

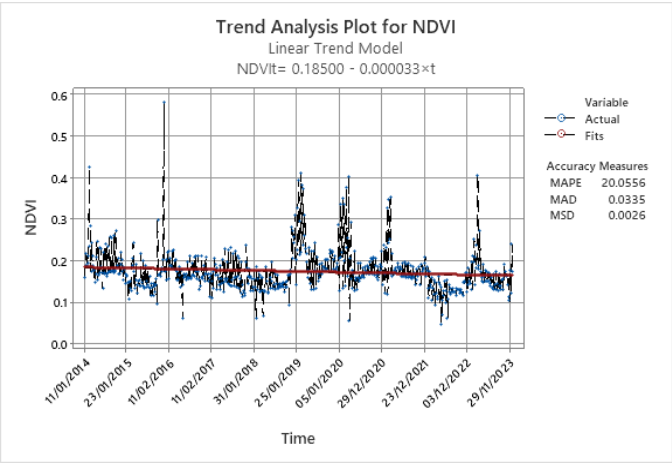

Figure 6. The NDVI observations and the linear regression equation.

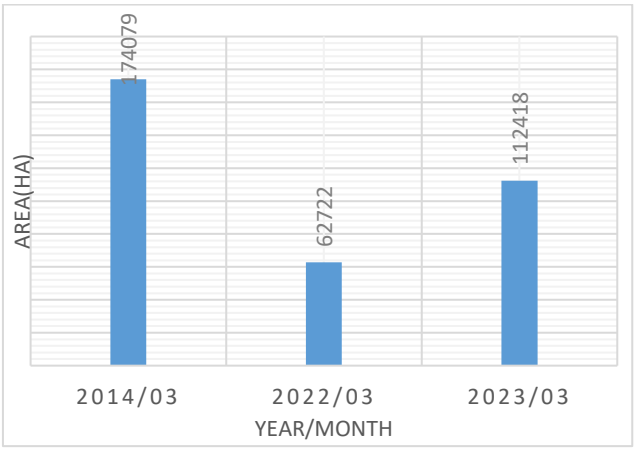

Figure 7. Areas of vegetation cover for reference (2022) years and forward and backward years

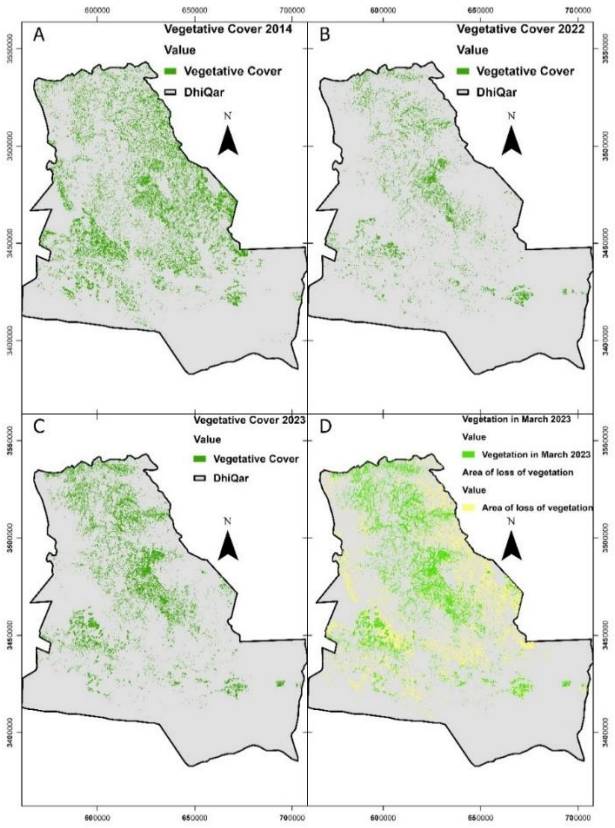

Figure 8. (A), (B), and (C) Distribution of vegetation cover in 2014,2022, and 2023, respectively, (D) Comparison between vegetation cover in 2023 and land that lost vegetation cover. (All figures are not to scale)

4. Conclusion

Three methods were used to analyze the NDVI time series in the study area of Dhi Qar, and the presence of a negative trend was confirmed. Using SLR and MK confirmed the presence of a negative trend in the NDVI value. Moreover, the BEAST model showed more accurate details in analysing the trend direction and change points in the NDVI time series. The negative trend of the NDVI value coincided with a lack of rainfall in the study area of Dhi Qar. We conclude that

meteorological drought severely affects the vegetation cover in the study area in Dhi Qar, as repeated meteorological drought leads to the loss of vegetation cover and, thus, land degradation.

Additionally, our secondary findings indicate that in 2019, the region experienced abundant rainfall, which correlated with an increase in vegetation density. This observation confirmed the sensitivity of vegetation cover to meteorological drought in that area. In 2022, the study area faced a substantial reduction in vegetation cover, which coincided with a decrease in rainfall. This situation was part of a global drought, underscoring the connection between vegetation cover changes in the study area and global climate change. To analyze the trend in the NDVI time series from 2014 to 2023, we employed three methods, all of which indicated a negative trend. However, the BEAST model proved to be the most effective, providing detailed insights into the trend, change points, extent of change, and direction of the slope.

Acknowledgment

We express our gratitude to the Iraqi Ministry of Agriculture, specifically the Dhi Qar Agriculture Directorate, for their invaluable assistance in providing us with the necessary information.

Conflict of interest

The authors declare that there are no conflicts of interest regarding the publication of this manuscript.

Author Contribution Statement

Mohammed H Azeez: developed the theory, performed the computations, and wrote the original draft preparation.

Hisham M. Jawad Al Sharaa and Abdul Razzak T. Ziboon proposed the research problem.

Hisham M. Jawad Al Sharaa and Abdul Razzak T. Ziboon verified the analytical methods and investigated and supervised the findings of this work.

All authors have read and agreed to the published version of the manuscript.

References

[1] K. Jiang et al., "Global land degradation hotspots based on multiple methods and indicators," *Ecol. Indic.*, vol. 158, p. 111462, 2024, doi: https://doi.org/10.1016/j.ecolind.2023.111462.

[2] J. Gambo et al., "Unveiling and modelling: Land degradation, poverty nexus in Nigeria's semi-arid (jigawa state) using cloud-based geospatial data," *J. Arid Environ.*, vol. 222, p. 105151, 2024, doi: https://doi.org/10.1016/j.jaridenv.2024.105151.

[3] R. S. Dwivedi, *Geospatial Technologies for Land Degradation Assessment and Management*. CRC Press, 2018.

[4] C. Zhao et al., "Accurate vegetation destruction detection using remote sensing imagery based on the three-band difference vegetation index (TBDVI) and dual-temporal detection method," *Int. J. Appl. Earth Obs. Geoinf.*, vol. 127, p. 103669, 2024, doi: https://doi.org/10.1016/j.jag.2024.103669.

[5] F. K. Aljanabi, M. Dedeoğlu, and C. Şeker, "Environmental Monitoring of Land Use/Land Cover by Integrating Remote Sensing and Machine Learning Algorithms," *J. Eng. Sustain. Dev.*, vol. 28, no. 4, pp. 455–466, 2024, doi: https://doi.org/10.31272/jeasd.28.4.4.

[6] T. Kirsten et al., "A regional, remote sensing-based approach to mapping land degradation in the Little Karoo, South Africa," *J. Arid Environ.*, vol. 219, p. 105066, 2023, doi: https://doi.org/10.1016/j.jaridenv.2023.105066.

[7] R. A. C. Torres et al., "Temporal analysis of land degradation and urban expansion in central Yunnan Province using remote sensing for supporting sustainable development goals 11/15," *Ecol. Indic.*, vol. 163, p. 112058, 2024, doi: https://doi.org/10.1016/j.ecolind.2024.112058.

[8] V. Bär, F. O. Akinyemi, and C. I. Speranza, "Land cover degradation in the reference and monitoring periods of the SDG Land Degradation Neutrality Indicator for Switzerland," *Ecol. Indic.*, vol. 151, p. 110252, 2023, doi: https://doi.org/10.1016/j.ecolind.2023.110252.

[9] A. Ziboon, M. Albayati, and F. Dalhel, "Monitoring Soil Degradation in The Mesopotamian Plain Using GIS and Remote sensing Techniques," *Eng. Technol. J.*, vol. 40, no. 5, pp. 649–660, 2022, doi: https://doi.org/10.30684/etj.v40i5.2121.

[10] R. Attafi et al., "Comparative analysis of NDVI and CHIRPS-based SPI to assess drought impacts on crop yield in Basrah Governorate, Iraq," *Casp. J. Environ. Sci.*, vol. 19, no. 3, pp. 547–557, 2021.

[11] I. Hatem et al., "Assessment of agricultural drought in Iraq employing Landsat and MODIS imagery," *Open Eng.*, vol. 14, no. 1, 2024, doi: https://doi.org/10.1515/eng-2022-0583.

[12] M. Rasheed, "Detection of the Impact of Climate Change on Desertification and Sand Dunes Formation East of the Tigris River in Salah Al-Din Governorate Using Remote Sensing Techniques," *Iraqi Geol. J.*, vol. 54, no. 1A, pp. 69–83, 2021, doi: https://doi.org/10.46717/igj.54.1A.7Ms-2021-01-28.

[13] M. R. Abbas, B. B. Ahmad, and T. R. Abbas, "Vegetation cover trends in Iraq for the period 2000-2012 using remote sensing technique," in *The 1st Academic Symposium on Integrating Knowledge Negeri*, 2014.

[14] H. M. Hassan and H. S. Dakheel, "Using the Normalized Difference Vegetation Index (NDVI) to study the change of vegetation cover in Thi-Qar Governorate, southern Iraq for the period from 1990-2022," *Texas J. Agric. Biol. Sci.*, vol. 13, pp. 72–84, 2023.

[15] W. M. Hashoush, "Detection of land cover changes in Dhi Qar Governorate for the period 3013-2020 using spectral indicators," *Univ. Thi-Qar J.*, vol. 11, no. 2, 2021.

[16] E. L. Bunting, S. M. Munson, and J. B. Bradford, "Assessing plant production responses to climate across water-limited regions using Google Earth Engine," *Remote Sens. Environ.*, vol. 233, p. 111379, 2019, doi: https://doi.org/10.1016/j.rse.2019.111379.

[17] M. Ali, A. Al-Adili, and N. Sivakugan, "Comparison Between Deterministic and Stochastic Interpolation Methods for Predicting Ground Water Level in Baghdad," *Eng. Technol. J.*, vol. 36, no. 12A, pp. 1222–1225, 2018, doi: https://doi.org/10.30684/etj.36.12A.2.

[18] M. R. T. Dale and M.-J. Fortin, *Spatial Analysis: A Guide for Ecologists*. Cambridge Univ. Press, 2014.

[19] K. Zhao et al., "Detecting change-point, trend, and seasonality in satellite time series data to track abrupt changes and nonlinear dynamics: A Bayesian ensemble algorithm," *Remote Sens. Environ.*, vol. 232, p. 111181, 2019, doi: https://doi.org/10.1016/j.rse.2019.04.034.

[20] G. V. Laurin et al., "Comparing ground below-canopy and satellite spectral data for an improved and integrated forest phenology monitoring system," *Ecol. Indic.*, vol. 158, p. 111328, 2024, doi: https://doi.org/10.1016/j.ecolind.2023.111328.

[21] Y. N. Scarpetta et al., "BFASTm-L2, an unsupervised LULCC detection based on seasonal change detection – An application to large-scale land acquisitions in Senegal," *Int. J. Appl. Earth Obs. Geoinf.*, vol. 121, p. 103379, 2023, doi: https://doi.org/10.1016/j.jag.2023.103379.

[22] F. Di Nunno, G. de Marinis, and F. Granata, "Analysis of SPI index trend variations in the United Kingdom – A cluster-based and 641ayesian ensemble algorithms approach," *J. Hydrol. Reg. Stud.*, vol. 52, p. 101717, 2024, doi: https://doi.org/10.1016/j.ejrh.2024.101717.

[23] S. Mehri, A. A. Alesheikh, and A. Lotfata, “Abiotic factors impact on oak forest decline in Lorestan Province, Western Iran,” *Sci. Rep.*, vol. 14, no. 1, p. 3973, 2024, doi: https://doi.org/10.1038/s41598-024-54551-6.

[24] A. Ganji et al., “Air pollution prediction and backcasting through a combination of mobile monitoring and historical on-road traffic emission inventories,” *Sci. Total Environ.*, vol. 915, p. 170075, 2024, doi: https://doi.org/10.1016/j.scitotenv.2024.170075.

[25] E. Saghbiny et al., “Breach Detection in Spine Surgery Based on Cutting Torque,” *IEEE Trans. Med. Robot. Bionics*, p. 1, 2024, doi: https://doi.org/10.1109/TMRB.2024.3421543.

[26] R. Lyu et al., “The impacts of disturbances on mountain ecosystem services: Insights from BEAST and Bayesian network,” *Appl. Geogr.*, vol. 162, p. 103143, 2024, doi: https://doi.org/10.1016/j.apgeog.2023.103143.

[27] M. Sakizadeh, A. Milewski, and M. T. Sattari, “Analysis of Long-Term Trend of Stream Flow and Interaction Effect of Land Use and Land Cover on Water Yield by SWAT Model and Statistical Learning in Part of Urmia Lake Basin, Northwest of Iran,” *Water*, vol. 15, no. 4, 2023, doi: https://doi.org/10.3390/w15040690.

[28] T. Hu et al., “Package ‘Rbeast’,” Dec. 08, 2023, v. 1. Accessed: Jul. 20, 2024. [Online]. Available: https://pypi.org/project/Rbeast/

[29] D. Ge, X. Gao, and W. Xinguang, "Changes in spatiotemporal drought characteristics from 1961 to 2017 in northeastern maize-growing regions, China," *Irrig. Sci.*, vol. 42, p. 3, 2023, doi: https://doi.org/10.1007/s00271-023-00893-4.

[30] V. K. Oad et al., "Time series analysis and impact assessment of the temperature changes on the vegetation and the water availability: A case study of Bakun-Murum Catchment Region in Malaysia," *Remote Sens. Appl.*, vol. 29, p. 100915, 2023, doi: https://doi.org/10.1016/j.rsase.2022.100915.

[31] C. R. de Almeida et al., "Time-series analyses of land surface temperature changes with Google Earth Engine in a mountainous region," *Heliyon*, vol. 9, no. 8, p. e18846, 2023, doi: https://doi.org/10.1016/j.heliyon.2023.e18846.

[32] M. Guo et al., “Detecting Global Vegetation Changes Using Mann-Kendal (MK) Trend Test for 1982–2015 Time Period,” *Chin. Geogr. Sci.*, vol. 28, pp. 907–919, 2018, doi: https://doi.org/10.1007/s11769-018-1002-2.

[33] M. Rhif et al., "Optimal selection of wavelet transform parameters for spatio-temporal analysis based on non-stationary NDVI MODIS time series in the Mediterranean region," *ISPRS J. Photogramm. Remote Sens.*, vol. 193, pp. 216–233, 2022, doi: https://doi.org/10.1016/j.isprsjprs.2022.09.007.

[34] Z. Wang et al., "Spatiotemporal characteristics and natural forces of grassland NDVI changes in Qilian Mountains from a sub-basin perspective," *Ecol. Indic.*, vol. 157, p. 111186, 2023, doi: https://doi.org/10.1016/j.ecolind.2023.111186.

[35] N. Neeti and J. R. Eastman, "A Contextual Mann-Kendall Approach for the Assessment of Trend Significance in Image Time Series," *Trans. GIS*, vol. 15, no. 5, pp. 599–611, 2011, doi: https://doi.org/10.1111/j.1467-9671.2011.01280.x.

[36] Z. S. Venter et al., "Application of Landsat-derived vegetation trends over South Africa: Potential for monitoring land degradation and restoration," *Ecol. Indic.*, vol. 113, p. 106206, 2020, doi: https://doi.org/10.1016/j.ecolind.2020.106206.

[37] S. Motiee, H. Motiee, and A. Ahmadi, "Analysis of rapid snow and ice cover loss in mountain glaciers of arid and semi-arid regions using remote sensing data," *J. Arid Environ.*, vol. 222, p. 105153, 2024, doi: https://doi.org/10.1016/j.jaridenv.2024.105153.

[38] R. M. Moreira, B. C. dos Santos, and R. G. Sanches, "Trend analysis of precipitation for protected areas and pasturelands in southwest Amazônia between 1998 and 2019," *Remote Sens. Appl.*, vol. 29, p. 100901, 2023, doi: https://doi.org/10.1016/j.rsase.2022.100901.

[39] R. O. Chávez et al., "Andean peatlands at risk? Spatiotemporal patterns of extreme NDVI anomalies, water extraction, and drought severity in a large-scale mining area of Atacama, northern Chile," *Int. J. Appl. Earth Obs. Geoinf.*, vol. 116, p. 103138, 2023, doi: https://doi.org/10.1016/j.jag.2022.103138.

[40] M. Sciortino et al., "Remote sensing for monitoring and mapping Land Productivity in Italy: A rapid assessment methodology," *Catena*, vol. 188, p. 104375, 2020, doi: https://doi.org/10.1016/j.catena.2019.104375.

[41] Md. Hussain and I. Mahmud, “pyMannKendall: a python package for non-parametric Mann Kendall family of trend tests,” *J. Open Source Softw.*, vol. 4, no. 39, p. 1556, 2019, doi: https://doi.org/10.21105/joss.01556.

[42] Z. T. Abdulrazzaq, R. H. Hasan, and N. A. Aziz, "Integrated TRMM data and standardized precipitation index to monitor the meteorological drought," *Civ. Eng. J.*, vol. 5, no. 7, pp. 1590–1598, 2019.

[43] I. A. Alwan and N. A. Aziz, "Monitoring of surface ecological change using remote sensing technique over Al-Hawizeh Marsh, Southern Iraq," *Remote Sens. Appl.*, vol. 27, p. 100784, 2022, doi: https://doi.org/10.1016/j.rsase.2022.100784.

[44] B. S. Shnichal, F. F. Lahmood, and R. A. M. Amin, "Use of Analytical Hierarchy Process (AHP) and Palmer Drought Severity Index (PDSI) to detect drought patterns (Dhi Qar-Iraq) study case," *J. Psychol. Engl.*, vol. 230, no. 1, pp. 1–14, 2022, doi: https://doi.org/10.5281/zenodo.6989257.